Available online at www.sciencedirect.com
ScienceDirect
Tetrahedron 64 (2008) 2824–2831
Tetrahedron
www.elsevier.com/locate/tet

Substituent effects in selenoxide elimination chemistry

Phoebe E. Macdougall [a,b], Naomi A. Smith [a,b], Carl H. Schiesser [a,b,*]

[a] School of Chemistry, The University of Melbourne, Victoria 3010, Australia
[b] Bio21 Molecular Science and Biotechnology Institute, The University of Melbourne, Victoria 3010, Australia

Received 1 October 2007; received in revised form 17 December 2007; accepted 10 January 2008
Available online 16 January 2008

Abstract

2α-(Arylseleno)cholestan-3-ones (**3**), 2α-(arylseleno)cholest-4-en-3-ones (**4**), and 4β-(arylseleno)-24-nor-5β-cholan-3-ones (**5**) were prepared and their stabilities toward oxidative elimination assessed. Simple competitive experiments demonstrate that electron-withdrawing substituents stabilize arylselenides toward oxidation, while electron-donating groups accelerate the oxidation process. In addition, ab initio and density functional calculations on model systems reveal that selenoxides are relatively insensitive to the nature of substituents on selenium toward elimination, suggesting that the oxidation step is rate-determining during oxidative elimination of selenides. Some results for sulfur and tellurium are also presented.

1. Introduction

The elimination of selenoxides to form unsaturated linkages is firmly entrenched in the synthetic chemists' toolbox and there are many examples of the use of these transformations in the literature.[1] In the example given in Scheme 1, Thomas and co-workers used this chemistry to prepare a key intermediate (**1**) during work toward the synthesis of the antiparasitic compound, milbemycin G.[2]

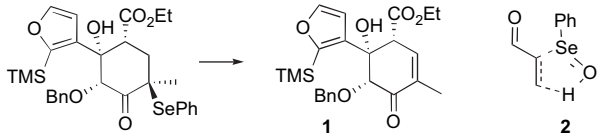

Scheme 1. Reagents and conditions: 30% aq H_2O_2, CH_2Cl_2 (50%).

It is generally agreed that the mechanism of this transformation most likely involves oxidation of the selenide to the corresponding oxide followed by rapid elimination via a cyclic transition state (**2**), and there are computational studies that support this hypothesis.[3,4]

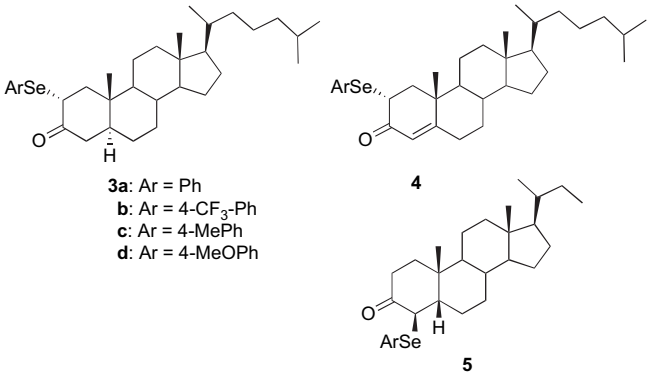

As part of ongoing studies into selenium-containing therapeutic agents,[5–7] we need to prepare arylseleno derivatives (**3**–**5**) of 3-cholestanone, cholest-4-en-3-one, and 24-nor-5β-cholan-3-one that were reasonably stable to elimination under aerobic conditions. In principle, this outcome could be achieved by either slowing down the rate of oxidation of arylselenides (**3**–**5**) through judicious choice of aryl substituent, or by decreasing the rate of the elimination step itself (or both). We reasoned that electron-withdrawing substituents on the aryl group (e.g., CF_3) should decrease the rate of oxidation

* Corresponding author. Tel.: +61 3 8344 2432; fax: +61 3 9347 8189.
E-mail address: carlhs@unimelb.edu.au (C.H. Schiesser).

0040-4020/$ - see front matter © 2008 Elsevier Ltd. All rights reserved.
doi:10.1016/j.tet.2008.01.044

by reducing the electron density on selenium, while donating groups (e.g., MeO) should have the opposite effect (Scheme 2). However, it was less clear to us what effect, if any, these same groups would have on the elimination step itself.

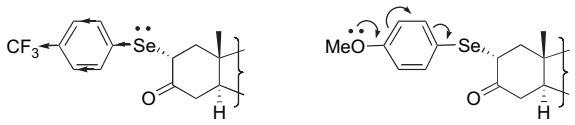

Scheme 2.

We now report the results of both laboratory and computational studies into the effects of substituents in selenoxide elimination chemistry. Simple competitive studies allow us to conclude that, in line with expectation, donating groups accelerate the oxidation step, while withdrawing groups stabilize these arylselenides toward oxidation. In addition, the effect of electron-withdrawing and donating groups on the ability of selenoxides to undergo concerted elimination was examined using computational techniques that also provide a comparison with the analogous processes involving sulfur and tellurium.

2. Results and discussion

2.1. Competitive oxidation studies

We began this work by preparing phenylseleno-substituted steroids (**3a**–**5a**). 2α-(Phenylseleno)cholestan-3-one (**3a**) was prepared from 3-cholestanone and isolated in 57% yield by treatment with phenylselenenyl chloride in ethyl acetate and could be separated from varying amounts of cholest-1-ene-3-one (**6**), the product of elimination, by flash chromatography (Scheme 3). Prepared in this manner, **3a** was identical to that reported previously.[8] In similar fashion, **4a** was isolated in 20% yield from cholest-4-ene-3-one, and after separation from cholesta-1,4-dien-3-one (**7**), proved to be identical to that prepared previously.[9]

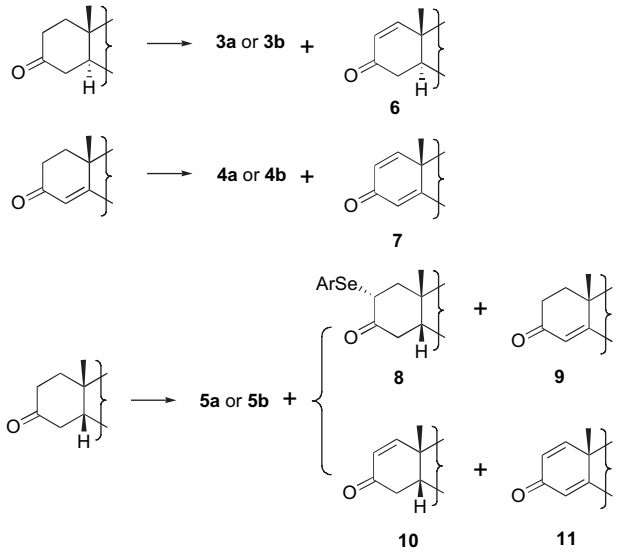

Scheme 3. Reagents and conditions: PhSeCl or 4-(CF_3)PhSeCl, EtOAc.

When 24-nor-5β-cholan-3-one,[10] prepared by the PCC oxidation of 24-nor-5β-cholan-3α-ol,[11] was reacted with phenylselenenyl chloride in ethyl acetate, 4β-(phenylseleno)-24-nor-5β-cholan-3-one (**5a**) was isolated in 49% yield after chromatographic separation from minor amounts of the 2β-isomer (**8**) and products (**9**–**11**) of elimination (Scheme 3).

The use of 4-(trifluoromethyl)phenylselenenyl chloride afforded the required compounds (**3b**–**5b**) in similar yields after chromatographic separation from the same sets of byproducts as was observed with phenylselenenyl chloride (Scheme 3).

When these reactions were repeated using (4-methoxyphenyl)selenenyl chloride, the only products observed were those (**6**, **7**, **9**–**11**) of elimination,[12] while 4-tolylselenenyl chloride led to mixtures in which the required products (**3c**–**5c**) appeared to be minor constituents as evidenced by ^{1}H NMR spectroscopy and were unable to be adequately purified by chromatography.

Based on these observations, one can tentatively conclude that the compounds bearing the more electron-rich arylseleno substituents (**3c**,**d**–**5c**,**d**) are more susceptible to aerobic oxidation and subsequent elimination than the 'parent' or electron-deficient selenides (**3a**,**b**–**5a**,**b**). This conclusion is further supported by simple competition studies involving **3a**,**b** and **5a**,**b**. For example, after an NMR solution containing an equimolar amount of **3a** and **3b** in $CDCl_3$ was allowed to sit in contact with 10 mol % hydrogen peroxide (as a 30% aqueous solution) for 72 h, ^{1}H NMR spectroscopy revealed signals at δ 5.84 and 7.14 characteristic of cholest-1-ene-3-one (**6**).[13] Importantly, the ratio of the signals at δ 4.26 and 4.16 corresponding to H-2 in **3b** and **3a**, respectively, was observed to be 1.7, indicating that the trifluoromethyl substituted system (**3b**) is less susceptible to oxidation and subsequent elimination than the 'parent' steriod (**3a**). This ratio increased to 2.4 after 96 h. Similar results were observed for competition studies involving **4a**/**4b**.[14] We conclude that electron-withdrawing groups on the arylseleno substituent offer some protection against aerobic oxidation and elimination, at least for the systems in this study.

2.2. Computational studies

In order to determine the effect, if any, that groups of varying electron demand have on the elimination step itself, we chose to use ab initio and density functional (DFT) techniques, initially on simple systems (**12**) derived from 3-(methylseleno)butanone (Scheme 4). This system would also afford us the opportunity to benchmark various computational methods.

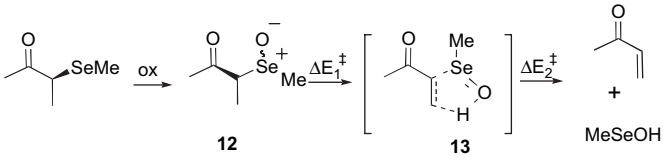

Scheme 4.

It should be noted that oxidation of racemic 3-(methylseleno)butanone will lead to a pair of *erythro* (*R*,*S*:*S*,*R*) and

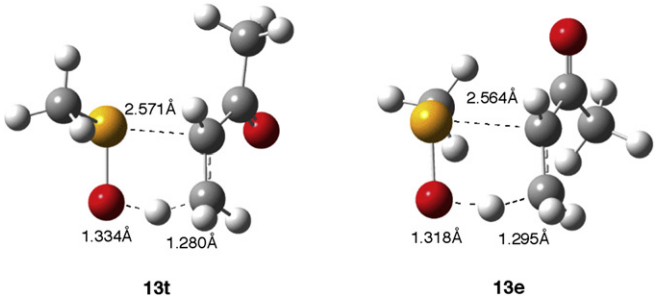

Figure 1. B3LYP/6-311G** optimized structures of transition states **13t**, **13e** involved in the oxidative elimination of 3-(methylseleno)butanone.

a pair of *threo* (*R*,*R*:*S*,*S*) diastereomeric selenoxides that need to be considered separately from a computational perspective.[15]

Searching of the $C_5H_{10}SeO_2$ potential energy surface located two diastereomeric selenoxides (**12**). The *erythro* structure (**12e**) proved to be higher in energy than the corresponding *threo* structure (**12t**) at all levels of theory used in this study. At the B3LYP/6-311G** level, the difference in energies is calculated to be only 3.4 kJ mol^{-1} and this small difference would lead to an approximately 4:1 ratio of **12t** over **12e** at ambient temperature, assuming thermodynamic control. More likely, the oxidation is under kinetic control and would lead to an approximately equal distribution of selenoxides (**12**).

Further examination of the surface located cyclic transition states **13t**,**e** for elimination in the *threo* and *erythro* manifolds, respectively. These structures proved to be true transition states as evidenced by one imaginary frequency in the harmonic frequency set, and were the lowest energy transition structures found through conformational searching. The B3LYP/6-311G** structures of both isomers of **13** are displayed in Figure 1. Full details at all levels of theory used in this study are available as Supplementary data. It is interesting to note that while **13t** is derived from the *anti* conformation of **12**, the lowest energy conformation of **13e** has the *syn* configuration. It should also be noted that the corresponding MP2/6-311G** structures are slightly 'later' than that calculated at B3LYP, with the key distances in **13t**, for example, calculated to be 2.440, 1.305, and 1.288 Å. These distances compare favorably with those calculated by Fujimoto and co-workers for simple methylselenides at low levels of theory,[3] and Bayse and Allison for similar reactions involving selenocysteine.[4]

Table 1 lists the calculated energy barriers ($\Delta E_1^{\ddagger}$, $\Delta E_2^{\ddagger}$, Scheme 4) for the forward and reverse reactions involving the *threo* isomer. As is clearly evident from the data in Table 1, in the absence of electron correlation, high barriers are predicted for the forward and reverse reactions, with values of $\Delta E_1^{\ddagger}$ in excess of about 150 kJ mol^{-1}. When electron correlation is included (MP2), $\Delta E_1^{\ddagger}$ drops to about 70 kJ mol^{-1}, however, single-point higher-order correction increases this value by about 14 kJ mol^{-1} using CCDS(T).

At the B3LYP/6-311G** level of theory, $\Delta E_1^{\ddagger}$ is further reduced to about 65 kJ mol^{-1}. The data in Table 1 also reveal that smaller basis sets like cc-pVDZ also reduce $\Delta E_1^{\ddagger}$. It is possible that the QCISD and CCSD(T) geometries are sufficiently

Table 1
Calculated energy barriers ($\Delta E_1^{\ddagger}$, $\Delta E_2^{\ddagger}$) for the forward and reverse elimination reactions involving **12t** and imaginary frequency (ν) associated with transition state **13t** (Scheme 4)

Level	$\Delta E_1^{\ddagger}$ [a]	$\Delta E_1^{\ddagger}$ + ZPE [a]	$\Delta E_2^{\ddagger}$ [a]	$\Delta E_2^{\ddagger}$ + ZPE [a]	ν [b]
RHF/6-31G*	171.1	156.2	187.1	180.3	1897i
RHF/6-311G**	157.3	142.5	229.5	222.5	1850i
RHF/cc-pVDZ	149.2	—	227.3	—	—
RHF/aug-cc-pVDZ	163.3	—	224.7	—	—
MP2/6-311G**	71.7	57.6	63.3	59.2	798i
QCISD/6-311G**[c]	99.6	—	113.5	—	—
CCSD(T)/6-311G**[d]	85.5	—	93.1	—	—
B3LYP/6-311G**	64.8	51.0	90.8	84.8	976i
B3LYP/cc-pVDZ	55.5	—	83.0	—	—
B3LYP/aug-cc-pVDZ	66.0	—	91.3	—	—

[a] Energies in kJ mol^{-1}.
[b] Frequencies in cm^{-1}.
[c] QCISD/6-311G**//MP2/6-311G**.
[d] CCSD(T)/6-311G**//MP2/6-311G**.

different to those from MP2 and that these differences are responsible for the unusual (upward) trend observed when higher-order correlation is included. These data can be compared to those of Fujimoto; MP2/3-21G(*)//RHF/3-21G(*) calculations provide a value of 68.4 kJ mol^{-1} for the analogous elimination reaction involving the oxide of 1-methoxy-2-(methylseleno)propane.[3] Unfortunately this study did not provide product energy data.

It is also interesting to note that while most levels of theory predict that the elimination reaction involving **12t** is exothermic, MP2/6-311G** predicts a slightly endothermic reaction. On the basis of the data provided in Table 1, we conclude that the elimination of 3-butenone from **12t** is most likely an exothermic process with a (gas phase) energy barrier somewhere in the range 50–70 kJ mol^{-1}.

Energy data for the similar processes involving **12e** at selected levels of theory are provided in Table 2 and clearly indicate that, apart from 2–3 kJ mol^{-1} increase in both $\Delta E_1^{\ddagger}$ and $\Delta E_2^{\ddagger}$, the same trends are observed as were evident for the chemistry involving **12t**.

We next turned our attention to chemistry involving substituents of varying electron demand on selenium. To that end, we examined the chemistry of the oxides (**14**, **15**) of 3-(trifluoromethylseleno)butanone and 3-(aminoseleno)butanone, molecules bearing electron-withdrawing and donating groups, respectively (Scheme 5). Guided by the data obtained for the methylselenides (above) and with the aim of getting a qualitative picture of the effects of substituents on selenium, we

Table 2
Calculated energy barriers ($\Delta E_1^{\ddagger}$, $\Delta E_2^{\ddagger}$) for the forward and reverse elimination reactions involving **12e** and imaginary frequency (ν) associated with transition state **13e** (Scheme 4)

Level	$\Delta E_1^{\ddagger}$ [a]	$\Delta E_1^{\ddagger}$ + ZPE [a]	$\Delta E_2^{\ddagger}$ [a]	$\Delta E_2^{\ddagger}$ + ZPE [a]	ν [b]
RHF/6-31G*	174.9	159.2	190.1	183.0	1894i
RHF/6-311G**	159.8	144.2	232.8	225.3	1708i
MP2/6-311G**	73.5	61.4	67.1	64.1	853i
B3LYP/6-311G**	65.7	53.3	95.0	90.0	1056i

[a] Energies in kJ mol^{-1}.
[b] Frequencies in cm^{-1}.

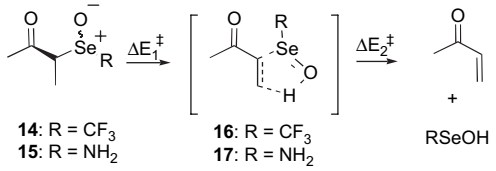

Scheme 5.

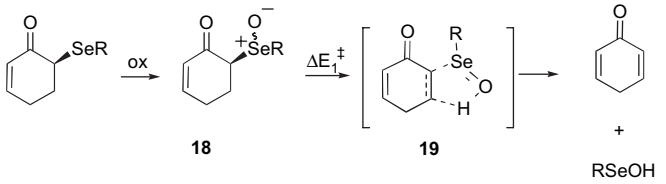

Scheme 6.

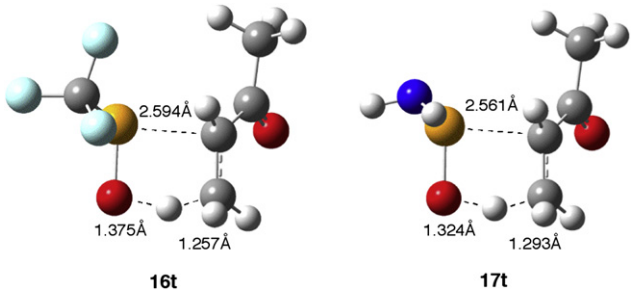

Figure 2. B3LYP/6-311G** optimized structures of transition states **16t**, **17t** involved in the oxidative elimination of **14t**, **15t**.

chose to only examine the *threo* reaction manifold involving these systems. Figure 2 displays the transition states (**16t**, **17t**) involved in each transformation depicted in Scheme 5, while Table 3 lists the associated energy barriers at selected levels of theory.

As is clearly evident in Figure 2, replacement of the methyl group in **13t** with either trifluoromethyl (**16t**) or amino (**17t**) has little effect on the critical distances in the cyclic transition states for elimination. The data in Table 3 show similar trends to those previously discussed as the levels of theory are changed. Most interesting is the observation that at all levels of theory, the electron-withdrawing (CF_3) group has a slight lowering effect on $\Delta E_1^{\ddagger}$ (B3LYP: 3.4 kJ mol^{-1}) while the donating group (NH_2) has a more significant (B3LYP: 12.1 kJ mol^{-1}) raising effect on this barrier. These data, together with our experimental observations, allow us to conclude that substituent demand on the selenium atom appears to work in opposite directions in the oxidation and elimination steps that occur during selenoxide elimination chemistry.

Table 3
Calculated energy barriers ($\Delta E_1^{\ddagger}$, $\Delta E_2^{\ddagger}$) for the forward and reverse elimination reactions involving **14** and **15** and imaginary frequency (ν) associated with transition states **16** and **17** (Scheme 5)

	$\Delta E_1^{\ddagger}$ [a]	$\Delta E_1^{\ddagger}$ + ZPE[a]	$\Delta E_2^{\ddagger}$ [a]	$\Delta E_2^{\ddagger}$ + ZPE[a]	ν [b]
14t, **16t**					
RHF/6-31G*	159.6	144.6	193.2	185.9	1790i
RHF/6-311G**	144.8	130.2	234.5	227.2	1678i
MP2/6-311G**	70.8	59.2	72.3	69.5	803i
B3LYP/6-311G**	61.4	49.5	94.4	89.2	830i
15t, **17t**					
RHF/6-31G*	183.7	168.8	188.1	181.2	1915i
RHF/6-311G**	169.1	154.5	228.2	221.1	1876i
MP2/6-311G**	86.3	73.5	64.0	57.0	881i
B3LYP/6-311G**	76.9	63.7	92.8	86.1	1055i

[a] Energies in kJ mol^{-1}.
[b] Frequencies in cm^{-1}.

In order to provide data for systems that more closely resemble the compounds that were part of our experimental study, we next examined the analogous elimination chemistry in conjugated ring systems that bear methyl- and phenylseleno substituents (Scheme 6) using B3LYP/6-311G**. Once again, this chemistry involves diastereomeric pairs of oxides (**18**) and transition states (**19**) and, as we observed in the other systems in this study, the *R*,*R*:*S*,*S* (*threo*) pair of oxides (**18**) proved to be of lower overall energy and were therefore the *threo* reaction manifold was chosen as representative of this chemistry.

Calculated energy barriers ($\Delta E_1^{\ddagger}$) for the elimination step itself are listed in Table 4, while a representative transition state (**19t**, R=Ph) is displayed in Figure 3. Full details of all structures are available as Supplementary data.

As is clearly evident from these data, these cyclic systems eliminate with energy barriers some 11 kJ mol^{-1} lower than those associated with the parent structures (**12**). Somewhat surprising, both methyl and phenyl substituents are predicted to react with the essentially the same values of $\Delta E_1^{\ddagger}$, namely 55 kJ mol^{-1}.

Finally, we chose to examine the effect of chalcogen in this chemistry and consequently examined elimination reactions involving the sulfur (**20t**) and tellurium (**21t**) analogues of

Table 4
B3LYP/6-311G** calculated energy barriers ($\Delta E_1^{\ddagger}$) for the elimination reactions involving **18t** and imaginary frequency (ν) associated with transition states **19t** (Scheme 6)

R	$\Delta E_1^{\ddagger}$ [a]	$\Delta E_1^{\ddagger}$ + ZPE[a]	ν [b]
Me	55.3	42.3	937i
Ph	55.6	42.0	919i

[a] Energies in kJ mol^{-1}.
[b] Frequencies in cm^{-1}.

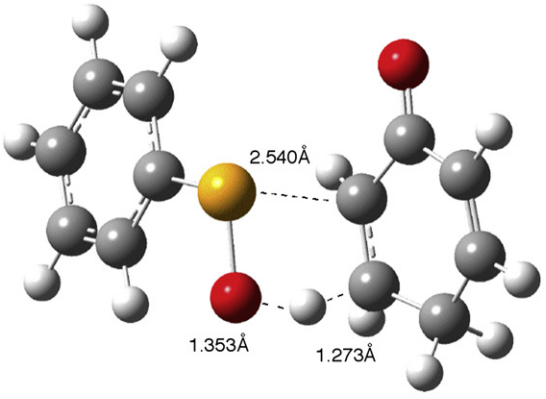

Figure 3. B3LYP/6-311G** optimized structures of transition state **19t** (R=Ph) involved in the oxidative elimination of **18t** (R=Ph).

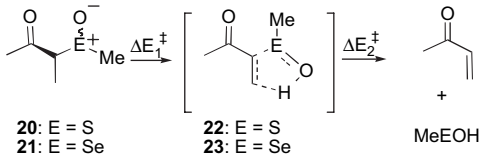

20: E = S
21: E = Se
22: E = S
23: E = Se

Scheme 7.

12t (Scheme 7). Once again, calculated energy barriers ($\Delta E_1^{\ddagger}$, $\Delta E_2^{\ddagger}$) are provided in Table 5, with calculated transition structures (**22t**, **23t**) displayed in Figure 4.

Unfortunately, for the higher heteroatoms such as tellurium reliable all-electron basis sets are not available mainly because of relativistic factors operating in the core region of the atom. Pseudopotential basis sets offer a solution to this issue and we have previously employed these in calculations involving tellurium, iodine, and tin. The DZP basis set (see below) has been shown by us to provide similar data as those generated by 6-311G** and we consider it reliable for our purposes.[16]

As expected, the data in Table 5 shows that sulfoxide eliminations proceed less readily than their selenium counterparts, with a B3LYP/6-311G** value of 84.6 kJ mol^{-1} for $\Delta E_1^{\ddagger}$ involving transition state **22t**, some 20 kJ mol^{-1} higher that calculated for the corresponding selenoxide. Similarly, telluroxide eliminations are calculated to be more favorable, for example, the MP2/DZP value for $\Delta E_1^{\ddagger}$ for **21t** is some 15 kJ mol^{-1} lower than the corresponding MP2/6-311G** value calculated for **12t**.

Table 5
Calculated energy barriers ($\Delta E_1^{\ddagger}$, $\Delta E_2^{\ddagger}$) for the forward and reverse elimination reactions involving **20t** and **21t** and imaginary frequency (ν) associated with transition states **22t** and **23t** (Scheme 7)

	$\Delta E_1^{\ddagger}$[a]	$\Delta E_1^{\ddagger}$ + ZPE[a]	$\Delta E_2^{\ddagger}$[a]	$\Delta E_2^{\ddagger}$ + ZPE[a]	ν[b]
20t, **22t** (E=S)					
RHF/6-31G*	199.4	183.4	187.1	180.3	1826i
RHF/6-311G**	185.0	169.4	229.5	222.5	1831i
RHF/cc-pVDZ	173.3	—	227.3	—	—
RHF/aug-cc-pVDZ	186.2	—	224.7	—	—
MP2/6-311G**	100.0	84.7	63.3	59.1	946i
QCISD/6-311G**[c]	127.4	—	113.5	—	—
CCSD(T)/6-311G**[d]	111.9	—	93.1	—	—
B3LYP/6-311G**	84.6	70.2	90.8	84.8	1090i
B3LYP/cc-pVDZ	74.4	—	83.0	—	—
B3LYP/aug-cc-pVDZ	84.2	—	91.3	—	—
21t, **23t** (E=Te)					
RHF/DZP[e]	145.8	130.7	244.8	235.8	1878i
MP2/DZP[e]	57.6	46.1	64.7	60.3	779i
B3LYP/DZP[e]	58.6	46.5	96.2	89.8	1000i

[a] Energies in kJ mol^{-1}.
[b] Frequencies in cm^{-1}.
[c] QCISD/6-311G**//MP2/6-311G**.
[d] CCSD(T)/6-311G**//MP2/6-311G**.
[e] For definition of DZP, see text.

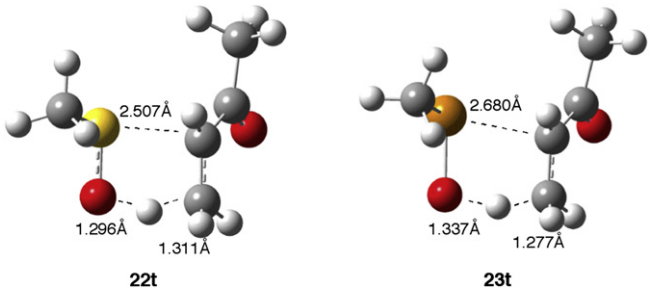

Figure 4. B3LYP/6-311G** optimized structures of transition state **22t**, and B3LYP/DZP optimized structure of transition state **23t**.

3. Conclusions

Simple competitive experiments have been used to demonstrate that electron-withdrawing substituents stabilize arylselenides toward oxidative elimination, while electron-donating groups accelerate the oxidation process. In addition, ab initio and density functional calculations on model systems reveal that selenoxides are relatively insensitive to the nature of substituents on selenium in the elimination step, suggesting that the oxidation step is rate-determining during oxidative elimination of selenides. These results allow for the design of selenides better matched to their oxidative environment.

4. Computational methods

Ab initio and DFT calculations were carried out on Dell PowerEdge 400SC computers using the Gaussian 03 program.[17] Geometry optimizations were performed using standard gradient techniques. All ground and transition states were verified by vibrational frequency analysis. Where appropriate, zero-point vibrational energy (ZPE) corrections have been applied. Standard basis sets were used, except for systems containing tellurium in which the (valence) double-ζ pseudopotential basis set of Hay and Wadt[18] supplemented with a single set of *d*-type polarization was used (exponent $d(\zeta)_{Te}$=0.252), together with the 6-311G** basis set for C, O, and H. We refer to this basis set as DZP throughout this work. Optimized geometries and energies for all structures of transition and ground states in this study (Gaussian Archive entries) are available as Supplementary data.

5. Experimental

5.1. General

Melting points are uncorrected. All NMR spectra were recorded in $CDCl_3$ on a Varian Inova 400 spectrometer. For ^{1}H the residual peak of $CHCl_3$ was used as the internal reference (δ 7.26) while the central peak of $CDCl_3$ (δ 77.0) was used as the reference for ^{13}C spectra. ^{77}Se NMR chemical shifts are given in parts per million relative to externally referenced diphenyl diselenide (δ 464). ^{19}F NMR chemical shifts are given in parts per million relative to externally referenced trifluoroacetic acid (δ −78.5). EI mass spectra were recorded at 70 eV on a Shimadzu QP5050 spectrometer. MS data are given for ^{80}Se. Tetrahydrofuran and diethyl ether were distilled under nitrogen from sodium/benzophenone. Flash chromatography was performed using Scharlau Kieselgel 60.

5.2. 24-Nor-5β-cholan-3-one[10]

To a solution of PCC (3.78 g, 17.6 mmol) in anhydrous CH_2Cl_2 (20.0 mL) was added 24-nor-5β-cholan-3α-ol[11] (3.89 g, 11.7 mmol) in CH_2Cl_2 (30.0 mL). The reaction mixture was stirred for 4.5 h at room temperature under nitrogen before Et_2O (200 mL) was added and the solution concentrated in vacuo. Flash chromatography (20% Et_2O/petroleum spirits) gave 24-nor-5β-cholan-3-one as a white solid (3.09 g, 96%). R_f (20% Et_2O/petroleum spirits) 0.32. ^{1}H NMR: δ 0.68 (s, 3H, 18-CH_3), 0.80–1.60 (m, 26H, CH and CH_2 of steroid skeleton), 1.79–1.89 (m, 3H, CH_3), 2.01–2.06 (m, 3H, CH_3), 2.13–2.18 (m, 1H, 2-CH), 2.29–2.34 (m, 1H, 2-CH), 2.70 (t(ap), 1H, 4-CH, J=14.3 Hz). ^{13}C NMR: δ 10.6, 12.4, 18.4, 21.5, 23.0, 24.5, 26.1, 26.9, 28.5, 28.6, 35.2, 35.8, 37.3, 37.3, 37.5, 40.4, 41.0, 42.7, 43.0, 44.7, 56.1, 56.7, 214.0. MS *m/z* (relative intensity) 330 (M^+, 27), 95 (31), 81 (44), 55 (100), 41 (75). IR ν_{max} 2931.0, 2867.1, 1737.5, 1713.9 cm^{-1}. Mp 140–142 °C, (lit.[11] 141–142 °C).

5.3. General procedure for the arylselenation of steroidal ketones

5.3.1. 2α-(Phenylseleno)cholestan-3-one (3a)[8]

To a solution of 3-cholestanone (200 mg, 0.518 mmol) in EtOAc (4.56 mL) was added phenylselenenyl chloride (120 mg, 0.621 mmol) under nitrogen. The reaction mixture was stirred for 1.0 h before being quenched with water (5 mL), extracted with EtOAc (3×10 mL), washed with water (3×10 mL), dried (Na_2SO_4), and the solvent was removed in vacuo. Flash chromatography (10% Et_2O/petroleum spirits) gave the title compound (**3a**) as a yellow gum (0.159 g, 57%). R_f (10% Et_2O/petroleum spirits) 0.17. ^{1}H NMR: δ 0.62–1.94 (m, 41H, CH and CH_2 of steroid skeleton), 2.24–2.41 (m, 3H, CH_3), 4.16 (dd, 1H, 2-CH, J=6.4 Hz, 13.0 Hz), 7.26 (d, 3H, $Ar_{3,4,5}$-CH, J=5.15 Hz), 7.52 (d, 2H, $Ar_{2,6}$-CH, J=8.45 Hz). ^{13}C NMR: δ 12.0, 12.0, 18.6, 21.3, 22.5, 22.8, 23.8, 24.2, 28.0, 28.2, 28.6, 31.5, 35.1, 35.7, 36.1, 37.6, 39.5, 39.7, 42.5, 44.6, 47.2, 48.0, 50.2, 53.6, 56.1, 56.2, 127.7, 128.3, 129.0, 134.8, 207.2. ^{77}Se NMR: δ 358.0. MS *m/z* (relative intensity) 542 (M^+, 12), 386 (1), 231 (18), 122 (32), 55 (57), 40 (100). IR ν_{max} 2971, 1739 cm^{-1}.

5.3.2. 2α-[4-(Trifluoromethyl)phenylseleno]cholestan-3-one (3b)

The title compound was prepared according to the general procedure using 3-cholestanone (100 mg, 0.260 mmol) in EtOAc (2.30 mL) and 4-(trifluoromethyl)phenylselenenyl chloride (81.1 mg, 0.312 mmol) in EtOAc (1.00 mL). Flash chromatography (10% Et_2O/petroleum spirits) afforded **3b** as a yellow gum (82.5 mg, 52%). R_f (10% Et_2O/petroleum spirits) 0.21. ^{1}H NMR: δ 0.64–2.46 (m, 44H, CH, CH_2 and CH_3 of steroid skeleton), 4.26 (dd, 1H, 2-CH, J=6.3 Hz, 13.2 Hz), 7.46 (d, 2H, $Ar_{2,6}$-CH, J=8.2 Hz), 7.60 (d, 2H, $Ar_{3,5}$-H, J=8.2 Hz). ^{13}C NMR: δ 12.0, 12.0, 18.6, 21.4, 22.5, 22.8, 23.8, 24.2, 28.0, 28.2, 28.6, 31.5, 35.1, 35.7, 36.1, 37.8, 39.5, 39.7, 42.5, 44.6, 47.4, 47.9, 50.3, 53.6, 56.1, 56.2, 124.3 (q, J_{CF}=272.4 Hz), 125.9 (q, J_{CF}=3.7 Hz), 126.3 (q, J_{CF}=3.7 Hz), 129.7 (q, J_{CF}=32.4 Hz), 134.0, 206.6. ^{19}F NMR: δ −65.2. ^{77}Se NMR: δ 362.2. MS *m/z* (relative intensity) 610 (M^+, 42), 55 (59), 43 (100). IR ν_{max} 2931, 2867, 1738, 1714 cm^{-1}. HRMS $(M+H)^+$ calcd for $C_{34}H_{49}F_3OSe$: 611.2974, found 611.2974.

5.3.3. 2α-(Phenylseleno)cholest-4-en-3-one (4a)[9]

The title compound was prepared according to the general procedure using cholest-4-en-3-one (100 mg, 0.260 mmol) in EtOAc (2.30 mL) and phenylselenenyl chloride (59.8 mg, 0.312 mmol). Flash chromatography (2.5% Et_2O/petroleum spirits) afforded **4a** as a yellow gum (27.4 mg, 20%). R_f (10% Et_2O/petroleum spirits) 0.11. ^{1}H NMR: δ 0.65 (s, 3H, 18-CH_3), 0.85–2.42 (m, 38H, CH, CH_2 and CH_3 of steroid skeleton), 4.24 (dd, 1H, 2-CH, J=4.8 Hz, 14.4 Hz), 5.80 (s, 1H, 4-CH), 7.28 (d, 3H, $Ar_{3,4,5}$-CH, J=1.5 Hz), 7.57 (d, 2H, $Ar_{2,6}$-CH, J=5.0 Hz). ^{13}C NMR: δ 12.2, 17.8, 18.9, 21.1, 22.9, 23.1, 24.1, 24.4, 28.3, 28.4, 30.0, 32.2, 32.9, 35.7, 36.0, 36.4, 39.8, 39.8, 41.0, 42.6, 44.7, 46.6, 54.1, 56.0, 56.3, 122.9, 128.0, 129.3, 135.2, 171.9, 196.1. ^{77}Se NMR: δ 366.4. MS *m/z* (relative intensity) 540 (M^+, 19), 197 (77), 122 (78), 55 (100). IR ν_{max} 2934, 2868, 1670 cm^{-1}.

5.3.4. 2α-[4-(Trifluoromethyl)phenylseleno]cholest-4-en-3-one (4b)

The title compound was prepared according to the general procedure using cholest-4-en-3-one (100 mg, 0.260 mmol) in EtOAc (2.30 mL) and 4-(trifluoromethyl)phenylselenenyl chloride (81.1 mg, 0.312 mmol) in EtOAc (1.00 mL). Flash chromatography (10% Et_2O/petroleum spirits) afforded **4b** as a yellow gum (56.3 mg, 36%). R_f (10% Et_2O/petroleum spirits) 0.17. ^{1}H NMR: δ 0.66–2.39 (m, 41H, CH, CH_2 and CH_3 of steroid skeleton), 4.33 (dd, 1H, 2-CH, J=4.8 Hz, 14.4 Hz), 5.83 (s, 1H, 4-CH), 7.50 (d, 2H, $Ar_{2,6}$-CH, J=7.1 Hz), 7.63 (d, 2H, $Ar_{3,5}$-CH, J=8.3 Hz). ^{13}C NMR: δ 11.8, 17.5, 18.6, 20.8, 22.5, 22.8, 23.8, 24.1, 28.0, 31.8, 32.7, 35.4, 35.7, 35.7, 36.0, 39.4, 39.4, 40.8, 42.3, 44.2, 46.6, 53.8, 55.7, 56.0, 122.4, 125.7 (q, J_{CF}=3.7 Hz), 126.0 (q, J_{CF}=3.7 Hz), 129.4 (q, J_{CF}=32.4 Hz), 133.7, 134.8, 171.8, 195.2. ^{19}F NMR: δ −65.2. ^{77}Se NMR: δ 371.7. MS *m/z* (relative intensity) 608 (M^+, 11), 527 (16), 265 (36), 122 (68), 55 (100). IR ν_{max} 2936, 2868, 1671, 1602.3 cm^{-1}. HRMS $(M+H)^+$ calcd for $C_{34}H_{47}F_3OSe$: 609.2817, found 609.2818.

5.3.5. 4β-(Phenylseleno)-24-nor-5β-cholan-3-one (5a)

The title compound was prepared according to the general procedure using 24-nor-5β-cholan-3-one (409 mg, 1.24 mmol) in EtOAc (10.9 mL) and phenylselenenyl chloride (285 mg, 1.49 mmol). Flash chromatography (10% Et_2O/petroleum spirits) afforded **5a** as a yellow gum (294 mg, 49%). R_f (10% Et_2O/petroleum spirits) 0.24. ^{1}H NMR: δ 0.61–2.86 (m, 36H, CH, CH_2 and CH_3 of steroid skeleton), 3.74 (d, 1H, 4-CH, J=7.8 Hz), 7.27 (d, 3H, $Ar_{2,4,6}$-CH, J=6.6 Hz), 7.56 (d, 2H, $Ar_{3,5}$-CH, J=6.6 Hz). ^{13}C NMR: δ 10.0, 11.6, 17.7, 21.0, 22.5, 23.8, 25.7, 26.0, 27.7, 27.9, 34.0, 34.3, 35.0, 35.7, 36.6, 39.4, 41.9, 42.2, 49.8, 52.7, 55.3, 55.7,

127.4, 127.9, 128.7, 134.8, 207.5. ^{77}Se NMR: δ 351.4. MS *m/z* (relative intensity) 485 (M^+, 8), 484 ($[M-H]^+$, 25), 95 (44), 81 (46), 55 (100). IR ν_{max} 2931, 2867, 1709 cm^{-1}. HRMS $(M+H)^+$ calcd for $C_{29}H_{42}OSe$: 487.2474, found 487.2474.

Also isolated were small amounts of 2α-(phenylseleno)-24-nor-5β-cholan-3-one (**8a**). ^{1}H NMR: δ 0.58–2.80 (m, 36H, CH, CH_2 and CH_3 of steroid skeleton), 4.18 (dd, 1H, 2-CH, *J*=5.27, 14.2), 7.25 (d, 2H, $Ar_{2,6}$-CH, *J*=4.5 Hz), 7.53 (d, 3H, $Ar_{3,4,5}$-CH, *J*=7.6 Hz). ^{13}C NMR: δ 10.2, 11.9, 18.0, 20.8, 22.2, 24.1, 25.7, 26.4, 28.0, 28.2, 35.4, 36.9, 37.2, 39.6, 41.1, 42.5, 45.2, 46.2, 49.7, 53.0, 55.6, 56.3, 127.7, 128.1, 128.9, 135.0, 208.6.

5.3.6. 4β-[4-(Trifluoromethyl)phenylseleno]-24-nor-5β-cholan-3-one (**5b**)

The title compound was prepared according to the general procedure using 24-nor-5β-cholan-3-one (100 mg, 0.303 mmol) in EtOAc (2.67 mL) and 4-(trifluoromethyl)phenylselenenyl chloride (81.1 mg, 0.312 mmol) in EtOAc (1.00 mL). Flash chromatography (5% Et_2O/petroleum spirits) afforded **5b** as a yellow gum (62.5 mg, 37%). R_f (10% Et_2O/petroleum spirits) 0.17. ^{1}H NMR: δ 0.65 (s, 3H, 18-CH_3), 0.79–1.59 (m, 25H, CH, CH_2 and CH_3 of steroid skeleton), 1.76–2.00 (m, 6H, CH, CH_2 and CH_3 of steroid skeleton), 2.32–2.41 (m, 1H, 2-CH), 2.57 2.62 (m, 1H, 2-CH), 3.90 (d, 1H, 4-CH, *J*=8.8 Hz), 7.48 (d, 2H, $Ar_{2,6}$-CH, *J*=8.20 Hz), 7.64 (d, 2H, $Ar_{3,5}$-CH, *J*=8.2 Hz). ^{13}C NMR: δ 10.3, 11.9, 18.0, 21.3, 22.9, 24.1, 26.0, 26.3, 28.0, 28.2, 34.7, 34.9, 35.3, 36.2, 36.9, 39.7, 42.2, 42.5, 50.2, 53.2, 55.6, 56.1, 124.0 (q, J_{CF}=271.7 Hz), 125.6 (q, J_{CF}=3.7 Hz), 126.1 (q, J_{CF}=3.7 Hz), 129.7 (q, J_{CF}=32.4 Hz), 134.1, 207.4. ^{19}F NMR: δ −65.2. ^{77}Se NMR: δ 358.1. MS *m/z* (relative intensity) 554 (M^+, 31), 95 (45), 81 (47), 55 (100). IR ν_{max} 2936, 2869, 1738, 1716.5 cm^{-1}. HRMS $(M+H)^+$ calcd for $C_{30}H_{41}F_3OSe$: 555.2348, found 555.2346.

5.3.7. 24-Nor-5β-cholan-4-en-3-one (**9**),[14] 24-nor-5β-cholan-1-en-3-one (**10**), and 24-nor-5β-cholan-1,4-dien-3-one (**11**)[10]

To a solution of 24-nor-5β-cholan-3-one (100 mg, 0.303 mmol) in EtOAc (2.67 mL) was added phenylselenenyl chloride (69.6 mg, 0.364 mmol) under nitrogen. The reaction mixture was stirred for 1 h before being washed with water (5 mL). The organic phase was returned to a reaction vessel, THF (1.2 mL) added, followed by the dropwise addition of 30% hydrogen peroxide (75 μL). The reaction mixture was stirred for 2.5 h, before being washed with water (5 mL), satd Na_2CO_3 (5 mL), dried ($MgSO_4$), and the solvent removed in vacuo. Flash chromatography (15% Et_2O/petroleum spirits) afforded **10** (25.7 mg, 26%), **9** (18.2 mg, 18%), and **11** (13.9 mg, 14%) as a white crystalline solid. Compound **10**: mp 93–95 °C. R_f (15% Et_2O/petroleum spirits) 0.25. ^{1}H NMR: δ 0.68 (s, 3H, 18-CH_3), 0.78–2.13 (m, 31H, CH, CH_2 and CH_3 of steroid skeleton), 2.72–2.81 (m, 1H, 4-CH), 5.89 (d, 1H, 2-CH, *J*=10.1 Hz), 6.84 (d, 1H, 1-CH, *J*=10.3 Hz). ^{13}C NMR: δ 10.3, 12.0, 18.0, 20.9, 22.3, 24.2, 26.0, 26.5, 27.9, 28.2, 35.2, 36.9, 38.6, 39.0, 39.8, 41.0, 42.6, 46.2, 55.7, 55.7, 126.9, 161.8, 201.0. MS *m/z* (relative intensity) 328 (M^+, 13), 122 (100), 109 (59), 79 (68), 55 (82), 41 (73). IR ν_{max} 2932, 2869, 1679, 1614 cm^{-1}. HRMS $(M+H)^+$ calcd for $C_{22}H_{36}O$: 329.2839, found 329.2839. Compound **9**:[14] mp 160–164 °C. R_f (15% Et_2O/petroleum spirits) 0.11. ^{1}H NMR: δ 0.71 (s, 3H, 18-CH_3), 0.80–2.04 (m, 27H, CH, CH_2 and CH_3 of steroid skeleton), 2.23–2.47 (m, 5H, CH, CH_2 and CH_3 of steroid skeleton), 5.72 (s, 1H, 4-CH). ^{13}C NMR: δ 10.3, 11.9, 17.4, 18.0, 21.0, 24.1, 28.0, 28.2, 29.7, 32.0, 32.9, 34.0, 35.6, 36.9, 38.6, 39.6, 42.3, 53.8, 55.5, 55.8, 123.7, 171.9, 199.8. MS *m/z* (relative intensity) 328 (M^+, 15), 229 (23), 124 (100), 79 (52), 55 (80), 41 (76). IR ν_{max} 2933, 2870, 1727, 1675, 1617 cm^{-1}. Compound **11**:[10] mp 166–169 °C (lit.[10] 168–170 °C). R_f (15% Et_2O/petroleum spirits) 0.07. ^{1}H NMR: δ 0.73 (s, 3H, 18-CH_3), 0.80–2.06 (m, 26H, CH, CH_2 and CH_3 of steroid skeleton), 2.33–2.47 (m, 2H), 6.07 (s, 1H, 4-CH), 6.23 (d, 1H, 1-CH, *J*=10.1 Hz), 7.06 (d, 1H, 2-CH, *J*=10.3 Hz). ^{13}C NMR: δ 10.0, 11.7, 17.6, 18.3, 22.5, 24.0, 27.6, 27.9, 29.4, 32.6, 33.4, 35.2, 36.6, 39.1, 42.3, 43.4, 52.1, 55.1, 55.2, 123.4, 127.0, 155.9, 186.2. MS *m/z* (relative intensity) 326 (M^+, 3), 122 (100), 91 (40), 79 (27), 55 (69), 41 (77). IR ν_{max} 2938, 2869, 1727, 1664, 1626, 1603 cm^{-1}.

Acknowledgements

The support of the Australian Research Council through the Centres of Excellence Program and the Victorian Institute for Chemical Sciences High Performance Computing Facility is gratefully acknowledged.

Supplementary data

Optimized geometries and energies of structures **12–23** as Gaussian Archive Entries. Supplementary data associated with this article can be found in the online version, at doi:10.1016/j.tet.2008.01.044.

References and notes

1. Jones, D. N.; Mundy, D.; Whitehouse, R. D. *J. Chem. Soc., Chem. Commun.* **1970**, 86–88; Sharpless, K. B.; Lauer, R. F. *J. Am. Chem. Soc.* **1973**, *95*, 2697–2699; Sharpless, K. B.; Lauer, R. F. *J. Org. Chem.* **1974**, *39*, 429–430; Reich, H. J. *Acc. Chem. Res.* **1979**, *12*, 22–30. For further examples see: Back, T. G. *The Chemistry of Organic Selenium and Tellurium Compounds*; Patai, S., Ed.; Wiley: Chichester, UK, 1987; Vol. 2, pp 91–213.
2. Bailey, S.; Helliwell, M.; Teerawutgulrag, A.; Thomas, E. J. *Org. Biomol. Chem.* **2005**, *3*, 3654–3677.
3. Kondo, N.; Fueno, H.; Fujimoto, H.; Makino, M.; Nakaoka, H.; Aoki, I.; Uemura, S. *J. Org. Chem.* **1994**, *59*, 5254–5263.
4. Bayse, C. A.; Allison, B. D. *J. Mol. Model.* **2007**, *13*, 47–53.
5. Carland, M. W.; Martin, R. L.; Schiesser, C. H. *Org. Biomol. Chem.* **2004**, *2*, 2612–2618.
6. Aumann, K. M.; Scammells, P. J.; White, J. M.; Schiesser, C. H. *Org. Biomol. Chem.* **2007**, *5*, 1276–1281.
7. Grange, R. L.; Ziogas, J.; Angus, J. A.; Schiesser, C. H. *Tetrahedron Lett.* **2007**, *48*, 6301–6303.
8. Back, T. G.; Birss, V. I.; Edwards, M.; Krishna, M. V. *J. Org. Chem.* **1988**, *53*, 3815–3822.

9. Blumbach, J.; Hammond, D. A.; Whiting, D. A. *J. Chem. Soc., Perkin Trans. 1* **1986**, 261–268.
10. Barton, D. H. R.; Boivin, J.; Crich, D.; Hill, C. H. *J. Chem. Soc., Perkin Trans. 1* **1986**, 1805–1808.
11. Schiesser, C. H.; Skidmore, M. A.; White, J. M. *Aust. J. Chem.* **2001**, *54*, 199–204.
12. Identified in the ^{1}H NMR spectrum of the crude reaction mixture by comparison with authentic standards of **6**, **7**, **9**–**11**. Reactions were carried out under nitrogen. We presume that oxidation is occurring during work up of the reaction mixture.
13. Rubin, M.; Armbrecht, B. H. *J. Am. Chem. Soc.* **1953**, *75*, 3513–3516.
14. Under identical conditions, ratio of **4b/4a** was 2.3 (72 h) and 5.0 (96 h).
15. The terms *erythro* and *threo* are used here assuming that the stereogenic carbon atom maps onto C-2 of the aldotetrose carbohydrate, with the stereogenic selenium atom mapping onto C-3. This exercise leads to a reversal of substituent priorities on carbon from what is normal for carbohydrates.
16. Schiesser, C. H.; Wild, L. M. *Aust. J. Chem.* **1995**, *48*, 175–184; Schiesser, C. H.; Styles, M. L.; Wild, L. M. *J. Chem. Soc., Perkin Trans. 2* **1996**, 2257–2262; Schiesser, C. H.; Styles, M. L. *J. Chem. Soc., Perkin Trans. 2* **1997**, 2335–2340; Horvat, S. M.; Schiesser, C. H. *J. Chem. Soc., Perkin Trans. 2* **2001**, 939–945; Horvat, S. M.; Schiesser, C. H.; Wild, L. M. *Organometallics* **2000**, *19*, 1239–1246; Matsubara, H.; Horvat, S. M.; Schiesser, C. H. *Org. Biomol. Chem.* **2003**, *1*, 1199–1203; Matsubara, H.; Schiesser, C. H. *J. Org. Chem.* **2003**, *68*, 9299–9309; Matsubara, H.; Schiesser, C. H. *Org. Biomol. Chem.* **2003**, *1*, 4335–4341.
17. Frisch, M. J.; Trucks, G. W.; Schlegel, H. B.; Scuseria, G. E.; Robb, M. A.; Cheeseman, J. R.; Montgomery, J. A., Jr.; Vreven, T.; Kudin, K. N.; Burant, J. C.; Millam, J. M.; Iyengar, S. S.; Tomasi, J.; Barone, V.; Mennucci, B.; Cossi, M.; Scalmani, G.; Rega, N.; Petersson, G. A.; Nakatsuji, H.; Hada, M.; Ehara, M.; Toyota, K.; Fukuda, R.; Hasegawa, J.; Ishida, M.; Nakajima, T.; Honda, Y.; Kitao, O.; Nakai, H.; Klene, M.; Li, X.; Knox, J. E.; Hratchian, H. P.; Cross, J. B.; Adamo, C.; Jaramillo, J.; Gomperts, R.; Stratmann, R. E.; Yazyev, O.; Austin, A. J.; Cammi, R.; Pomelli, C.; Ochterski, J. W.; Ayala, P. Y.; MoroMelody Gabrielma, K.; Voth, G. A.; Salvador, P.; Dannenberg, J. J.; Zakrzewski, V. G.; Dapprich, S.; Daniels, A. D.; Strain, M. C.; Farkas, O.; Malick, D. K.; Rabuck, A. D.; Raghavachari, K.; Foresman, J. B.; Ortiz, J. V.; Cui, Q.; Baboul, A. G.; Clifford, S.; Cioslowski, J.; Stefanov, B. B.; Liu, G.; Liashenko, A.; Piskorz, P.; Komaromi, I.; Martin, R. L.; Fox, D. J.; Keith, T.; Al-Laham, M. A.; Peng, C. Y.; Nanayakkara, A.; Challacombe, M.; Gill, P. M. W.; Johnson, B.; Chen, W.; Wong, M. W.; Gonzalez, C.; Pople, J. A. *Gaussian 03, Revision B.05*; Gaussian: Pittsburgh, PA, 2003.
18. Wadt, W. R.; Hay, P. J. *J. Chem. Phys.* **1985**, *82*, 284–298; Hay, P. J.; Wadt, W. R. *J. Chem. Phys.* **1985**, *82*, 270–283; Hay, P. J.; Wadt, W. R. *J. Chem. Phys.* **1985**, *82*, 299–310.